

## Multiple-Pulse Sequences for Precise Transmitter Phase Alignment

A. J. SHAKA, D. N. SHYKIND, G. C. CHINGAS, AND A. PINES

*Department of Chemistry, University of California, Berkeley, California 94720, and Materials and Chemical Sciences Division, Lawrence Berkeley Laboratory, Berkeley, California 94720*

Received August 27, 1987; revised March 14, 1988

We show that arbitrary RF phase shifts can be measured precisely using the nuclear spins to monitor the phase of the RF field. Other imperfections like resonance offset, RF inhomogeneity, or symmetric phase transients are removed by the action of the multiple-pulse sequence and have little influence on the measurements. Phase shifts can be trimmed to the desired value with an uncertainty of less than 10 millidegrees in favorable cases. © 1988 Academic Press, Inc.

### INTRODUCTION

Many important NMR experiments require RF pulses of different phase, and phase shifters are now standard equipment on most all commercially available spectrometers. Two-dimensional experiments in liquids (1, 2) rely heavily on orderly phase cycles to select a certain signal while rejecting all others. In these experiments, errors in the RF phase shifts result in unwanted signal breakthrough and the appearance of artifacts. Composite pulses (3-12) can require rapid, accurate phase shifts of arbitrary values in order to operate successfully. Multiple-pulse experiments in solids (13-20) are notoriously sensitive to pulse imperfections, errors in the phase shifts included. Finally, multiple-quantum NMR (21-25), in which a phase error  $\Delta\phi$  propagates to  $n\Delta\phi$  for an  $n$ -quantum coherence, can prove very demanding as  $n$  becomes large.

In this paper we propose a straightforward method to set transmitter RF phase shifts to any desired value with high accuracy. The method, a generalization of the work of Haubenreisser and Schnabel (26), is reasonably insensitive to other imperfections such as RF inhomogeneity or resonance offset. It performs well in practice as we demonstrate by experiment. Using an oscilloscope, simple diagnostic patterns are produced for "rational" phase shifts of  $p\pi/q$  for small  $q$ , allowing quick trimming of the phase shifts to exactly the right values. More generally, Fourier transformation of the signal response allows the measurement and setting of arbitrary phase shifts. For systems in which the phase shifts are controlled by software, we can envision a scenario in which the computer automatically calibrates the phase shifts without operator intervention.

Symmetric and nonsymmetric versions of the basic sequence are shown in Fig. 1; they essentially differ only by the moment at which magnetization is sampled. Figure 1a becomes the Haubenreisser-Schnabel sequence when  $\phi = \pi/2$ , generating a net rotation about the  $y$  axis. The nonsymmetric sequence of Fig. 1b generates an equiva-

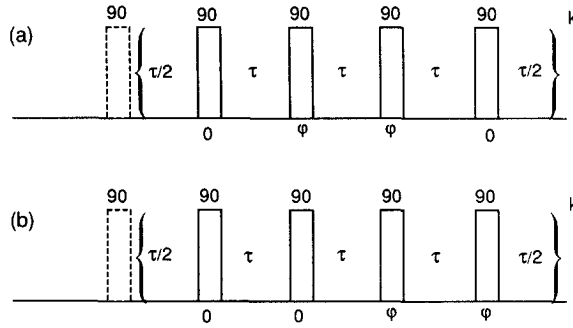


FIG. 1. Multiple-pulse sequences for phase alignment. Part (a) shows a symmetric repetitive sequence that gives a net rotation of  $2\phi$  about the  $-y$  axis. The corresponding nonsymmetric sequence of (b) delivers a net rotation about the  $z$  axis.

lent rotation about the  $z$  axis. The  $z$  rotation can be preferable for the Fourier transform experiment since only a single resonance is obtained. However, direct observation of the time-domain signal is simpler with the symmetric sequence, because it simplifies interaction with the receiver phase. For this reason, and to facilitate a comparison with earlier work (26), we concentrate on the symmetric version of the experiment.

#### THEORY

We consider the symmetric sequence of four  $90^\circ$  pulses applied to an ensemble of isolated spins, with the timing diagram shown in Fig. 1a. The first and last pulses are applied with a reference phase of 0, which may be considered  $+x$ , and the two center pulses are applied with relative phase  $\phi$ ,  $-\pi < \phi \leq \pi$ . The sequence may be preceded by a prepulse. For the on-resonance case, assuming perfectly rectangular pulses and neglecting relaxation, the result of the four-pulse sequence of Fig. 1a can be predicted exactly using rotation operators,

$$\begin{aligned} R &= R_x(\pi/2)R_z(\phi)R_x(\pi)R_{-z}(\phi)R_x(\pi/2) \\ &= R_{-y}(\phi)R_x(2\pi)R_{-y}(\phi), \end{aligned} \quad [1]$$

in which  $R_x(\alpha) \equiv \exp(-i\alpha I_x)$ , etc. The operator  $R_x(2\pi) = \pm 1$  depending on whether integer or half-integer spins are involved, so

$$R = \pm R_{-y}(2\phi). \quad [2]$$

Aside from the absolute sign of the operator, which we ignore hereafter, Eq. [2] shows that the result of the four-pulse sequence is a pure rotation of angle  $2\phi$  about the  $-y$  axis. If the four-pulse sequence is repeatedly applied and a single data point is captured after each segment, then we find for the  $x$  component of the magnetization  $\langle I_x(t) \rangle$  at integer multiples of  $\tau_c$

$$\langle I_x^s(n\tau_c) \rangle = \sin(2n\phi) \quad [3]$$

if the spins are initially prepared at thermal equilibrium, and

$$\langle I_x^c(n\tau_c) \rangle = \cos(2n\phi) \quad [4]$$

if they are initially prepared along the  $x$  axis of the rotating frame by a  $90_y^\circ$  prepulse. Fourier transformation of the cosine component determines  $2\phi$  modulo  $\pi$  up to a sign ambiguity, while if both components are available the sign of  $2\phi$  can be determined as well. Since the value of the phase shift is usually approximately known beforehand, either component can be used to determine  $\phi$ . The precision of the measurement depends on the number of data points that can be collected before the driven free induction decay is lost in the noise.

Equation [2] is only valid if the RF pulses are ideal, so it is very important to assess the likely impact of spectrometer imperfections on the phase calibration procedure. Our approach is to concentrate on the exact formula for the imperfections and then to recover the average Hamiltonian (13) result by expanding the error terms in a perturbation series. In this way the connection between the exact expressions and the average Hamiltonian approximation is made clear. One strategy we repeatedly employ is to express a product of small error rotations as a power series using the Baker–Campbell–Hausdorff formula:

$$\prod_k \exp(-i\delta_k \mathbf{m}_k \cdot \mathbf{I}) = \exp\left(-i\left\{\sum_k \delta_k \mathbf{m}_k \cdot \mathbf{I} + \frac{1}{2} \sum_{k>j} \delta_k \delta_j \mathbf{m}_k \times \mathbf{m}_j \cdot \mathbf{I} + \dots\right\}\right). \quad [5]$$

In Eq. [5] the  $\delta_k$  are small rotations about unit axes  $\mathbf{m}_k$  and the terms in the product on the left hand side are understood to be ordered with larger  $k$  to the left. The errors “cancel out” when the rotation they induce is nearly the identity operator. The algebraic conditions

$$\sum_k \delta_k \mathbf{m}_k = \mathbf{0} \quad [6]$$

$$\sum_{k>j} \delta_k \delta_j \mathbf{m}_k \times \mathbf{m}_j = \mathbf{0} \quad [7]$$

express this cancellation to first and second order in  $\delta$  which, rather confusingly, is referred to as zeroth or first order in the average Hamiltonian expansion. The other formula we need is the net rotation angle for a small rotation combined with a larger rotation. If  $\theta$  and  $\delta$  are arbitrary angles, and

$$\exp(-i\beta \mathbf{m}_3 \cdot \mathbf{I}) = \exp(-i\theta \mathbf{m}_2 \cdot \mathbf{I}) \exp(-i\delta \mathbf{m}_1 \cdot \mathbf{I}), \quad [8]$$

then  $\beta$  is given by

$$\cos(\beta/2) = \frac{1}{2} (1 + \mathbf{m}_1 \cdot \mathbf{m}_2) \cos\left(\frac{\theta + \delta}{2}\right) + \frac{1}{2} (1 - \mathbf{m}_1 \cdot \mathbf{m}_2) \cos\left(\frac{\theta - \delta}{2}\right). \quad [9]$$

If  $\mathbf{m}_1 = \pm \mathbf{m}_2$  then  $\beta = \theta \pm \delta$ , while if  $\mathbf{m}_1 \cdot \mathbf{m}_2 = 0$  and  $\delta$  is small,  $\beta \approx \theta$ . An important special case occurs for  $\theta = \pi$ , when  $\beta = \theta$  if  $\mathbf{m}_1 \cdot \mathbf{m}_2 = 0$  regardless of  $\delta$ .

We consider three sources of error: RF inhomogeneity, resonance offset, and symmetric phase transients. Of these, RF inhomogeneity has the greatest impact for liquid-state spectrometers employing saddle-coil configurations, while the symmetric phase transients could be more important for high-power applications in solids. Resonance offset is the least important imperfection since it is reasonable to assume that the frequency of the RF carrier can always be adjusted very near to resonance if a liquid sample such as water or acetone is used.

The rotation operator describing the four-pulse sequence in the presence of RF inhomogeneity, in which each spin experiences a flip angle  $\pi/2 + \epsilon(\mathbf{r})$  depending on its spatial position, can be written, for a single volume element,

$$R = R_x(\pi/2 + \epsilon)R_z(\phi)R_x(\pi + 2\epsilon)R_{-z}(\phi)R_x(\pi/2 + \epsilon) \quad [10]$$

which can be simplified to

$$R = R_{-y}(2\phi)R_\epsilon \quad [11]$$

with

$$R_\epsilon = [R_y(2\phi)R_x(\epsilon)R_{-y}(2\phi)][R_y(\phi)R_x(2\epsilon)R_{-y}(\phi)]R_x(\epsilon). \quad [12]$$

The grouping of the terms is meant to emphasize the “toggling-frame” transformation of the errors under the ideal rotation (13). Since the  $y$  rotations only act to tilt the axis of the  $\epsilon$  rotations into the  $xz$  plane, Eqs. [5] and [8] show that, provided  $2\phi$  dominates  $\epsilon$ ,  $R$  represents a rotation by an angle  $2\phi$  to first order in  $\epsilon$ . Thus, the error terms are quenched by the rotation induced by the phase difference between the pulses.

The same conclusion can be reached by using the average Hamiltonian method. In this case we select a rational phase shift  $\phi = p\pi/q$  and choose  $k$  so the  $2k\phi$  is a multiple of  $2\pi$ . This ensures that the sequence is cyclic in the average Hamiltonian sense. The exact formula for  $R_{k\epsilon}$  over the entire sequence becomes

$$R_{k\epsilon} = \exp(-i\epsilon I_x) \left\{ \prod_{n=2k-1}^1 \exp(-2i\epsilon[I_x \cos(n\phi) + I_z \sin(n\phi)]) \right\} \exp(-i\epsilon I_x). \quad [13]$$

Using Eq. [5] we find

$$R_{k\epsilon} = \exp\left\{-2i\left[\epsilon \sum_{n=0}^{2k-1} I_x \cos(n\phi) - I_z \sin(n\phi) + O(\epsilon^2)\right]\right\}. \quad [14]$$

The  $x$  and  $z$  components can be combined into a single complex version of Eq. [6]:

$$\sum_{n=0}^{2k-1} \exp(-in\phi) = 0. \quad [15]$$

Equation [15] is satisfied for all  $\phi \neq 0$ , because the sum is invariant to multiplication by  $\exp(i\phi)$ . In the case of an “irrational” phase shift, not of the form  $p\pi/q$ , the series must be extended to infinity (the sequence is never cyclic) but still becomes arbitrarily small. Paradoxically, *all* phase shifts other than zero appear to offer some compensation.

It should be remembered, however, that a power series offers a local description only. Even though all values  $\phi \neq 0$  produce an essentially parabolic dependence of  $2\phi$  on  $\epsilon$ , Eq. [15] gives no hint of the size of the second-order term, which in fact depends strongly on  $\phi$ . For  $\phi \neq 0$  we find, to second order,

$$R_{k\epsilon} = \exp\left\{2i\left[\epsilon^2 I_y \sum_{n=1}^{2k-2} (2k-1-n)\sin(n\phi) + O(\epsilon^3)\right]\right\}. \quad [16]$$

Equation [16] shows that values of  $\phi$  near  $\pi$ , for which the terms are all small and

alternate in sign, offer the best compensation. This conclusion should be geometrically obvious, for phase shifts near  $\pi$  cause the formation of rotary echoes that are insensitive to variations in the pulse flip angles. An inspection of the exact expression, Eq. [12], shows that  $R_c \rightarrow 1$  as  $\phi \rightarrow \pi$ . Accordingly, *all* terms in the average Hamiltonian expansion must vanish in this limit.

Equation [16] makes an important point: aside from the exceptional points  $\phi = 0$  and  $\phi = \pi$ , the effect of RF inhomogeneity is to *increase* the magnitude of the apparent rotation angle, *regardless of the sign of  $\epsilon$* . Because of this effect,  $|\phi|$  will be set to a slightly smaller value than desired.

To calculate resonance offset effects we use the  $\delta$ -pulse approximation, equivalent to neglecting the tilt of the effective field and slight lengthening of the  $\pi/2$  pulses (27) while still retaining the evolution due to free precession in the windows. If we assume a resonance offset  $\Delta\omega$  and let  $\delta = \Delta\omega\tau$  then, by the same procedure used for Eq. [10], we find

$$R = R_{-y}(2\phi)R_\delta, \quad [17]$$

where

$$R_\delta = [R_y(2\phi)R_{-z}(\delta/2)R_{-y}(2\phi)][R_y(\phi + \delta)R_z(\delta)R_{-y}(\phi + \delta)]R_{-z}(\delta/2). \quad [18]$$

Equations [5] and [8] again show that the error  $\delta$ , provided it is small, has no effect on the net rotation  $2\phi$  to first order in  $\delta$  unless  $\phi$  is close to  $\pi$  or an odd multiple thereof.

These assertions can be confirmed using the average Hamiltonian method. Using the same assumptions as before, the rotation operator for the cyclic sequence becomes

$$R_{k\delta} = \exp\left(i\frac{\delta}{2}I_z\right)\left[\prod_{n=k}^1 \exp(-i\delta[I_z\cos(\delta + (2n-1)\phi) + I_x\sin(\delta + (2n-1)\phi)])\right. \\ \left. \times \exp(i\delta[I_z\cos(2(n-1)\phi) + I_x\sin(2(n-1)\phi)])\right]\exp\left(-i\frac{\delta}{2}I_z\right). \quad [19]$$

The  $\delta$  terms in the arguments of the sine and cosine functions do not affect the first-order term in  $\delta$  and can be ignored. We then find

$$R_{k\delta} = \exp\left\{i\delta \sum_{n=1}^k I_z[\cos(2(k-1)\phi) - \cos((2k-1)\phi)]\right. \\ \left. + I_x[\sin(2(k-1)\phi) - \sin((2k-1)\phi)] + O(\epsilon^2)\right\} \quad [20]$$

which makes  $R_{k\delta}$  the identity operator to first order in  $\delta$  if

$$\sum_{n=0}^{2k-1} (-1)^n \exp(in\phi) = 0. \quad [21]$$

The sum is invariant to multiplication by  $\exp(2i\phi)$  and hence vanishes for all  $\phi$  except  $\phi = \pi$  or an odd multiple thereof. Higher-order terms with respect to resonance offset are irrelevant for the present discussion since we assume that  $\delta$  will be almost zero when the experiment is carried out.

The effect of symmetric phase transients can be modeled by replacing each RF pulse by a sandwich of three rotations

$$R_x(\pi/2) \rightarrow R_y(\beta)R_x(\pi/2)R_y(\beta) \quad [22]$$

and assuming that a phase shift transforms all three rotations in the same way as for a single pulse. The exact nature of the transients present in the experiment depends on the characteristics of the probe and RF circuitry, so that Eq. [22] is an oversimplification. Nevertheless, an analysis based on Eq. [22] can give some idea of the performance in an actual tuned circuit.

Proceeding exactly as before, we find

$$R = R_{-y}(2\phi)R_\beta, \quad [23]$$

where

$$R_\beta = R_y(\beta)[R_y(2\phi)R_z(\beta)R_{-y}(2\phi)][R_y(\phi)R_z(\beta)R_{-y}(2\beta)R_{-z}(\beta)R_{-y}(\phi)]R_{-z}(\beta)R_y(\beta). \quad [24]$$

Once again, Eqs. [5] and [8] show that  $R$  is a rotation of angle  $2\phi$  if  $2\phi$  dominates  $\beta$ . The error part for a cyclic sequence is

$$R_{k\beta} = \exp\left\{i\beta \sum_{n=0}^{k-1} I_z \{ \cos(2n\phi) - \cos(2(n+1)\phi) \} \right. \\ \left. + I_x \{ \sin(2n\phi) - \sin(2(n+1)\phi) \} + O(\beta^2) \right\} \quad [25]$$

which vanishes to first order in  $\beta$  if

$$\sum_{n=0}^{k-1} \exp(2in\phi) - \exp(2i(n+1)\phi) = 0. \quad [26]$$

The telescoping sum is an identity for all  $\phi$ , since  $\exp(2ik\phi) = 1$ . Inspection of the exact expression, Eq. [24], shows that  $R_\beta \rightarrow 1$  as  $\phi \rightarrow \pi$ . Symmetric phase transients thus show the same qualitative behavior as RF inhomogeneity with regard to  $\phi$ , except that the compensation is better near  $\phi = 0$ .

In summary, the errors induced by RF inhomogeneity or symmetric phase transients are increasingly compensated as  $\phi$  approaches  $\pi$ , while the tolerance to resonance offset effects is superior as  $\phi$  approaches 0. Operation on resonance allows all the offending terms to be removed by choosing values of  $\phi$  near enough to  $\pi$ .

#### PHASE CALIBRATION PROCEDURE

The first step in the phase calibration procedure is to balance the amplitudes between the channels. For this purpose, the sequence of Fig. 1 can be used with all four pulses set to the same phase, but with sampling after each  $90^\circ$  pulse, the so called "flip-flop" sequence. With the receiver reference phase correctly set, the periodically sampled time-domain signal gives rise to a pattern of three lines when  $\omega_1$  is set to the nominal value. A small deviation away from the  $90^\circ$  condition shows as a divergence of the central feature. Inhomogeneity of the RF field causes a decay of the observed magnetization; if the  $\omega_1$  distribution is symmetric about the nominal value the central

feature can still be nulled at all times, when the amplitude is correctly adjusted. In the case of a skewed distribution the central feature always shows some divergence and a compromise must be made (27). The important point is that all the channels should be adjusted to give the *same* pattern. If the phase and amplitude variables interact when the phase or amplitude of one channel is altered, it may be necessary to readjust the amplitudes after the phases have been adjusted, and proceed iteratively. Sequences are described in the literature for the measurement and characterization of any phase transients that may be present (28–30).

It is possible to calibrate rational phase shifts between the channels in essentially the same way as the amplitudes, by observing the patterns produced for the periodically sampled time-domain signal. A correctly adjusted phase shift of  $p\pi/q$ , where  $q > 2$  and  $p$  are relatively prime, gives a pattern of  $(q + 1)/2$  lines if  $q$  is odd, and  $(q + 2)/2$  lines if  $q$  is even, for the periodically sampled cosine component of Eq. [4]. The sine component, Eq. [3], gives  $q$  lines if  $q$  is odd,  $q/2$  lines if  $q$  is even and not a multiple of 4, and  $(q + 2)/2$  lines otherwise. Conversely, the observation of a  $k$ -line pattern for the cosine component limits  $q$  to  $2k - 1$  or  $2k - 2$ . The two cases can be distinguished by displaying only the odd-numbered time-domain data points. If  $q = 2k - 1$  then a  $k$ -line pattern results; if  $q = 2k - 2$  fewer lines will result, allowing the two cases to be distinguished. Confirmation is possible by displaying the sine component and verifying that the correct number of lines is obtained.

The special case of  $\pi/2$  phase shifts has been discussed by Haubenreisser and Schnabel (26). The sequence of Fig. 1a is used with  $\phi = \pi/2$ , without the initial prepulse. In this case it is advantageous to sample the magnetization at both the midpoint and the end of the four-pulse sequence, giving a three-line pattern. An error in the  $90^\circ$  phase shift shows up as a divergence of the central feature. This divergence is easier to identify visually than the incipient appearance of a cosine wave on a two-line pattern (produced with the prepulse *included*), since the latter can be hard to distinguish from the natural decay of the magnetization at the correct phase setting.

Suppose that  $2q$  phase shifts of  $\pi/q$  are to be systematically calibrated so that channel  $p$  has relative phase  $p\pi/q$ . This would be the case in a typical multiple-quantum experiment, for example. A phase shift *near*  $\pi$ , e.g.,  $(q - 1)\pi/q$ , is selected as the basic unit and calibrated between channels 0 and  $q - 1$ . For example, in the case of a series of  $45^\circ$  phase shifts, a  $135^\circ$  phase shift is established between channels 0 and 3 by adjusting channel 3 until the correct three-line pattern is obtained. The receiver reference phase is adjusted by  $135^\circ$  (by software) and the process repeated between channels 3 and 6. In the general case, each successive channel,  $n(q - 1) \bmod 2q$ , is then calibrated with respect to the first pair: channel  $2q - 2$  is adjusted until the same pattern is obtained between channels  $q - 1$  and  $2q - 2$ , etc., until  $n(q - 1) \bmod 2q$  is channel 0 again. If this last pair of channels also gives the correct pattern then all the phases are correctly set.

A significant systematic miscalibration shows up as a discrepancy on the last pair of channels, allowing a check on the procedure. In the example of  $45^\circ$  phase shifts, a series of  $3\pi/4 - \epsilon$  phase shifts results in a phase difference of  $3\pi/4 + 7\epsilon$  between the last pair of channels, which differs by  $8\epsilon$  from the other phase shifts and may be detectable even though the individual errors were not. By recording the initial setting of channel 0 and the setting ( $\sim -8\epsilon$ ) required to obtain a response congruent with

the other pairs of channels, channel 0 can be adjusted by approximately  $-\epsilon$ . The response between channels 0 and 3 is then recorded and taken to represent a  $135^\circ$  phase shift and the circuit is repeated. The remaining adjustments are then very small. It should not take more than one additional circuit to bring all the phases into alignment.

This check for self-consistency is of importance when very accurate calibration is desired, or if the RF field shows a wide distribution around the nominal value. As discussed earlier, the second-order term for RF inhomogeneity results in a slight increase in the apparent nutation frequency. A positive phase shift  $0 < \phi < \pi$  will thus be set to a somewhat *smaller* nominal value  $\phi - \xi$ , where  $\xi$  depends on the shape of the distribution, and on  $\phi$ . As we show in the experimental section, merely adjusting the phase shift to give a pattern closely resembling the naive prediction for the case of a perfectly homogeneous field keeps  $\xi$  typically well below  $0.1^\circ$  if the RF homogeneity is good. In contrast to the flip-flop sequence, the quadratic dependence on  $\epsilon$  expressed by Eq. [16] results in a compromise setting even if the RF distribution is symmetric.

The phase calibration is tedious when many channels are involved. The obvious solution is to use software control to trim the pulse amplitudes and phases. The procedure described here is repetitive enough that it can be programmed easily. All the phases could then be adjusted under computer control.

#### EXPERIMENTAL

Multiple-pulse free induction decays were obtained using a homebuilt spectrometer operating at 178.9 MHz for protons. This frequency was generated by mixing the output of a PTS 500 synthesizer with a 30 MHz intermediate frequency (IF), both of which were derived from the same 10 MHz clock. Transmitter phases were selected by apparatus normally used to generate quadrature pulses for multiple-pulse work (31, 32), acting on the IF. Four independently switched RF channels with mechanical amplitude and phase controls modified the 30 MHz IF prior to the final mixing stage to generate the Larmor frequency.

For these experiments the channels to be compared were first approximately aligned at the IF level using a Hewlett-Packard Model 8405A vector voltmeter. Only two channels were required for the experiments shown here, but three were generally checked for consistency. Two were kept in quadrature and the third was adjusted to the nonquadrature phase being investigated. After this preliminary adjustment, final calibration was performed by observing the NMR signal, using the familiar "flip-flop" sequence to set the amplitudes, and the new sequence described here to set the phases.

All experiments employed a single sample of heavily doped (0.01 M Cr(Acac)<sub>3</sub>) acetone in a 4 mm bulb housed within a sealed 30 mm length of 8 mm o.d. Pyrex tubing. The  $T_1$  for the proton resonance was approximately 200 ms; the field was shimmed to give a linewidth of less than 40 Hz. No field/frequency stabilization of the superconducting magnet was employed. The sample was centrally located within a 6 turn solenoid, 30 mm long and 8 mm in diameter. Flattened copper wire was used to improve the RF homogeneity across the sample. The probe coil was series



tuned for 178.9 MHz and matched, with a parallel capacitance, to  $50 \Omega$  to better than 10% reflected voltage. The quality factor for the matched resonance circuit was  $Q = 90$  at room temperature.

Radiofrequency power was supplied by a broadband ENI 5100L amplifier, capable of an output power of  $\sim 200$  W at 178.9 MHz. This proved sufficient to generate a field  $\omega_1/2\pi = 71.4$  kHz, giving a  $90^\circ$  pulse time of  $3.5 \mu\text{s}$ . An interpulse delay  $\tau = 40 \mu\text{s}$  provided an acceptable duty cycle while at the same time resulting in driven FIDs that decayed appreciably faster than would be expected due to relaxation alone. This allowed the predicted compensation for RF inhomogeneity to be verified experimentally. The relatively rapid decay under the flip-flop sequence could be empirically fitted quite closely by an  $\omega_1$  distribution consisting of a superposition of a Lorentzian distribution with a Lorentzian squared, both slightly skewed to lower field values. No theoretical significance is attributed to this particular functional form: it merely provided a simple means to simulate the expected decays for the phase calibration sequences.

The first trace of Fig. 2 shows the familiar three-line pattern, representing a nominal  $90^\circ$  phase shift, obtained with the sequence of Haubenreisser and Schnabel (26). Using the sequence of Fig. 1a without the initial prepulse, sampling of the  $x$  component of the magnetization occurs once at the midpoint of each four-pulse segment and once at the end. A total of 384 points are displayed for each multiple-pulse FID, corresponding to about 33.4 ms. By deliberately misadjusting the pulsewidth to  $3.6 \mu\text{s}$  ( $\alpha = 92.6^\circ$ ) and  $3.7 \mu\text{s}$  ( $\alpha = 95.1^\circ$ ) the tolerance to RF inhomogeneity can be monitored. An incipient slow oscillation on the outer features is evident for  $\alpha = 92.6^\circ$  and becomes considerably more pronounced for  $\alpha = 95.1^\circ$ .

The topmost trace of Fig. 3 shows the three-line pattern expected for a nominal  $45^\circ$  phase shift, sampling at the *end* of each four-pulse segment. The 384 points shown correspond to 66.8 ms, twice the length of the signals shown in Fig. 2. The small divergence of the central feature results from the RF inhomogeneity across the sample. As the  $90^\circ$  pulses are deliberately misadjusted, there is an increasingly rapid decay of the time-domain signal accompanied by faster oscillations. The oscillations can be slowed by misadjusting the phase shift as well, to a value slightly smaller than  $45^\circ$ . The exact value depends on how badly the pulses are in error. This behavior is in accord with the prediction of Eq. [16].

Figure 4 shows the simulated time-domain signals corresponding to the experimental data in Fig. 3, including the effects due to the  $\omega_1$  distribution, but neglecting relaxation. Closest agreement is obtained by supposing a phase shift  $\phi = 44.96^\circ$ . Simulations in which  $\phi$  varies by as little as  $0.01^\circ$  from this value give recognizably different behavior. Further simulations (not shown) were carried out to investigate the exact extent of the phase calibration error when the pulses are in error. Setting  $\alpha = 92.6^\circ$  gives a three-line pattern for  $\phi = 44.80^\circ$ , whereas  $\alpha = 95.1^\circ$  produces a three-line pattern for  $\phi = 44.20^\circ$ . Thus, with this rather narrow RF distribution, a  $2.6^\circ$  error in the flip angle results in a  $0.2^\circ$  phase error, while a  $5.1^\circ$  flip angle error gives a phase error of  $0.8^\circ$ .

Figure 5 demonstrates the superior compensation for RF inhomogeneity offered by a nominal  $135^\circ$  phase shift. Comparison with Fig. 3 shows that, even with the

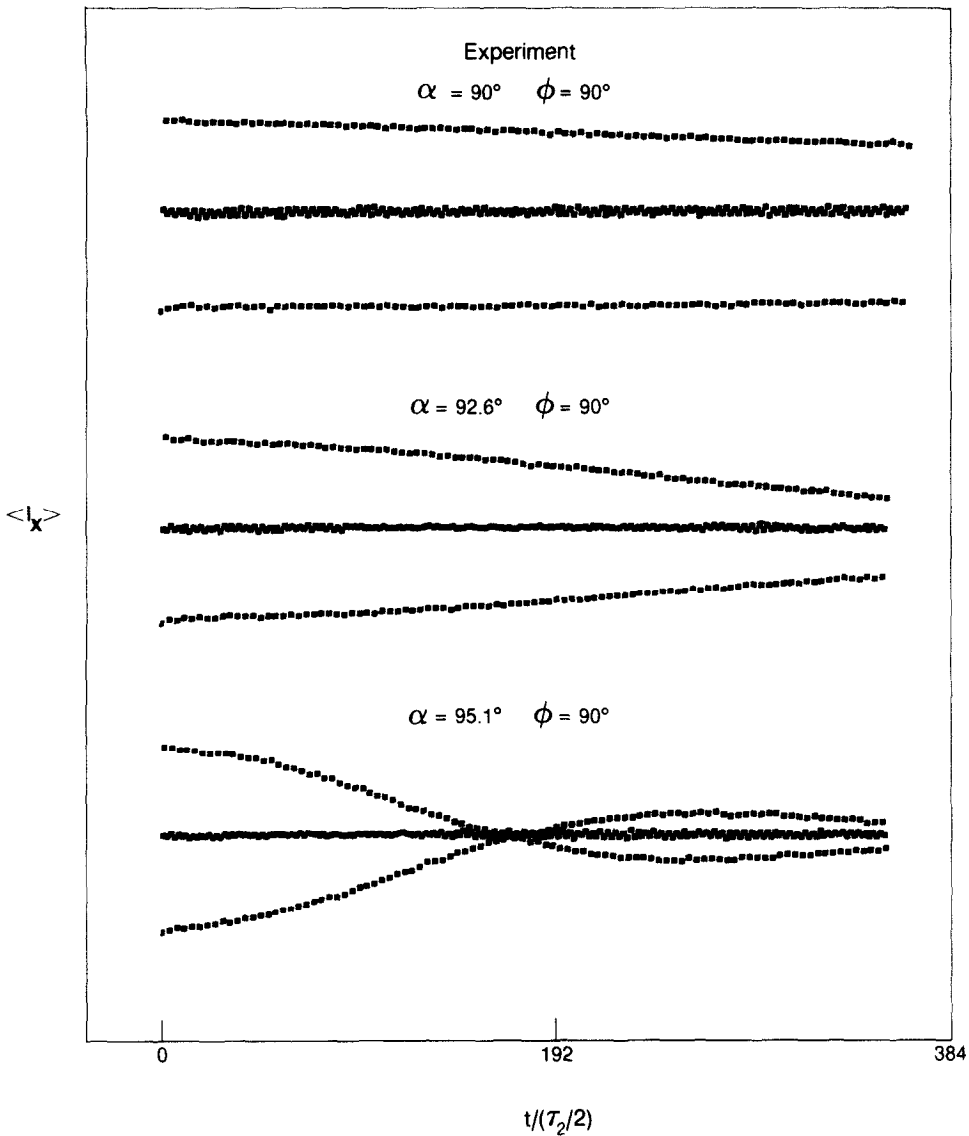


FIG. 2. Experimental results obtained with the sequence of Haubenreisser and Schnabel (26). A nominal  $90^\circ$  phase shift yields a three-line pattern when sampling occurs twice per period. Misadjustment of the  $90^\circ$  pulse lengths induces an oscillation on the outer features.

pulses badly misadjusted, long decays, having only very slow oscillations, are produced. In addition, with the pulses adjusted to  $\alpha = 90^\circ$ , there is less divergence of the central feature. It is therefore easier to make the correct adjustment visually. The simulations shown in Fig. 6 indicate a phase shift  $\phi = 134.987^\circ$  and are sensitive to changes as small as  $0.005^\circ$ . The noticeably larger amplitude near the end of the simulated signals is due to the neglect of relaxation in the calculation. The best three-line

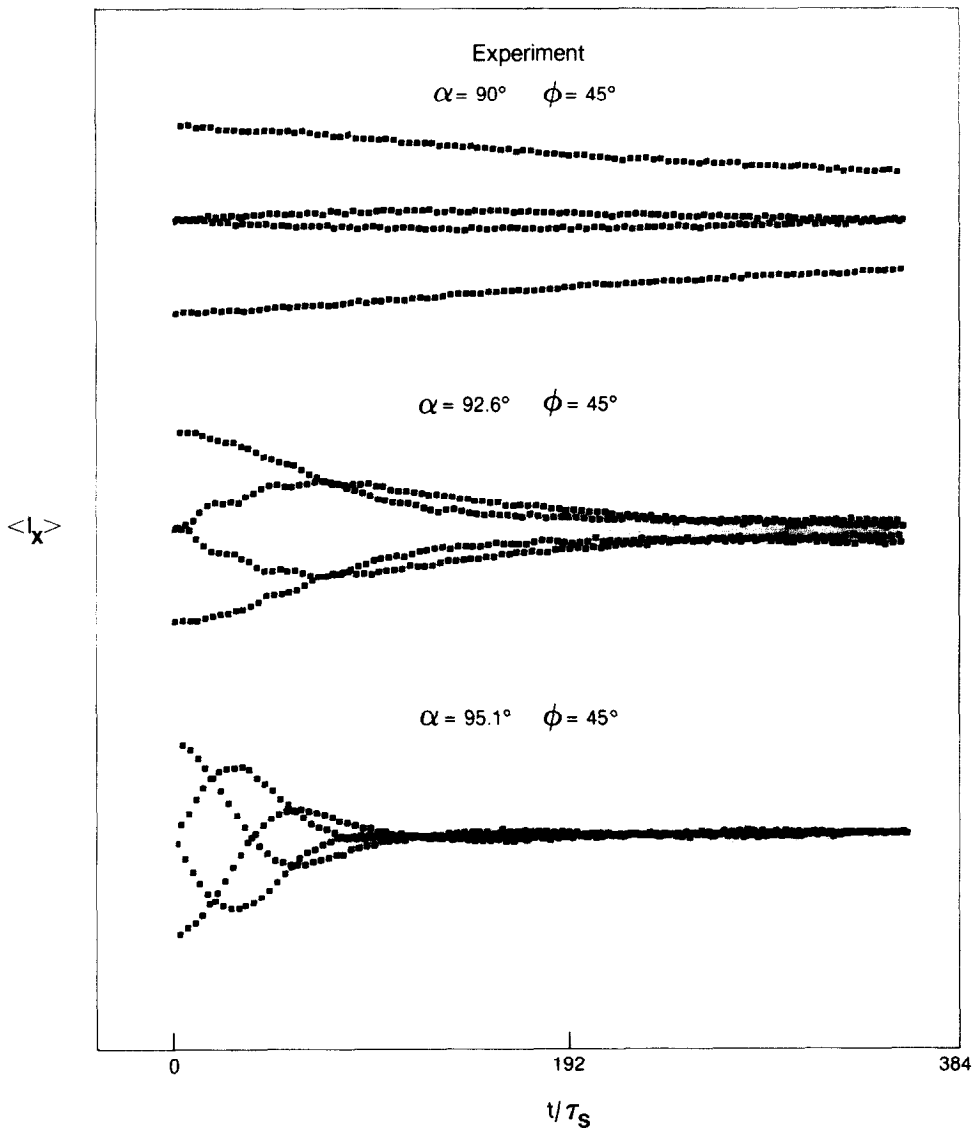


FIG. 3. Experimental results obtained with the sequence of Fig. 1a and a nominal  $45^\circ$  phase shift. The time-domain signal decays quickly when the  $90^\circ$  pulses are misadjusted, showing only limited compensation for RF inhomogeneity.

patterns (not shown) with the flip angles deliberately misadjusted are obtained with phase shifts of  $134.945^\circ$  ( $\alpha = 92.6^\circ$ ) and  $134.82^\circ$  ( $\alpha = 95.1^\circ$ ), errors of  $0.055^\circ$  and  $0.16^\circ$ , respectively.

We conclude this section with a demonstration of the patterns obtained for nominal phase shifts  $\phi = 112.5^\circ$  and  $\phi = 108^\circ$ , shown in Fig. 7. The  $112.5^\circ$  phase shift gives the pattern of five lines ( $p = 5$ ,  $q = 8$ ) expected for the sine component, Eq. [3]. A

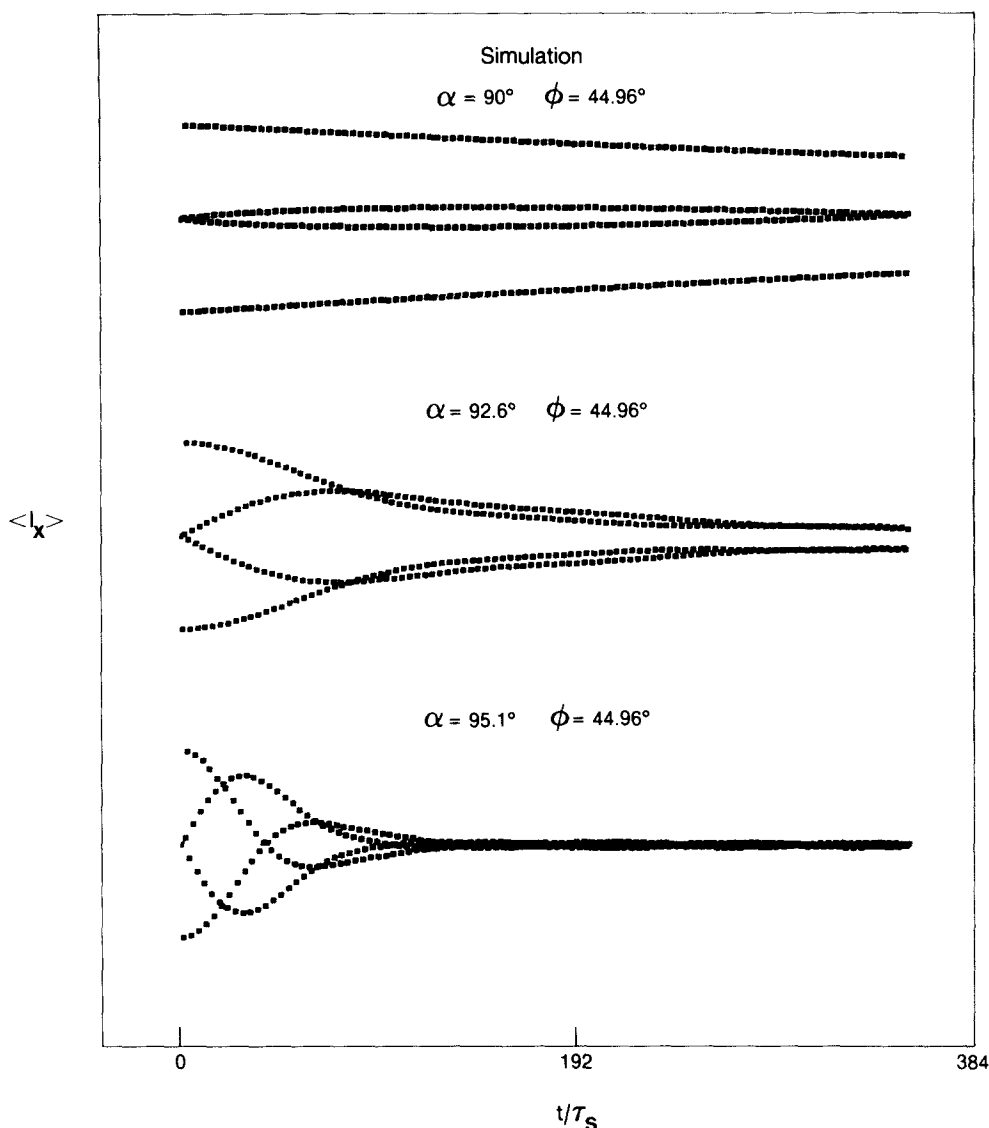


FIG. 4. Simulated multiple-pulse FIDs corresponding to the experimental data shown in Fig. 3. The RF field distribution across the test sample has been taken into account in the calculation, but relaxation has been neglected. Best agreement is obtained for a phase setting  $\phi = 44.96^\circ$ .

$108^\circ$  phase shift also gives a pattern of five lines ( $p = 3, q = 5$ ) in this case. The patterns are easily distinguishable in the figure, but are somewhat harder to identify from an oscilloscope trace alone. The simulations give the best agreement for the values  $\phi = 112.479^\circ$  and  $\phi = 107.98^\circ$ , respectively. The systematic error of about  $0.02^\circ$  is nearly the same for the two phase shifts because they are so close.

We have found that six- and seven-line patterns are very hard to identify on an oscilloscope trace, so smaller phase increments place greater demands on display res-

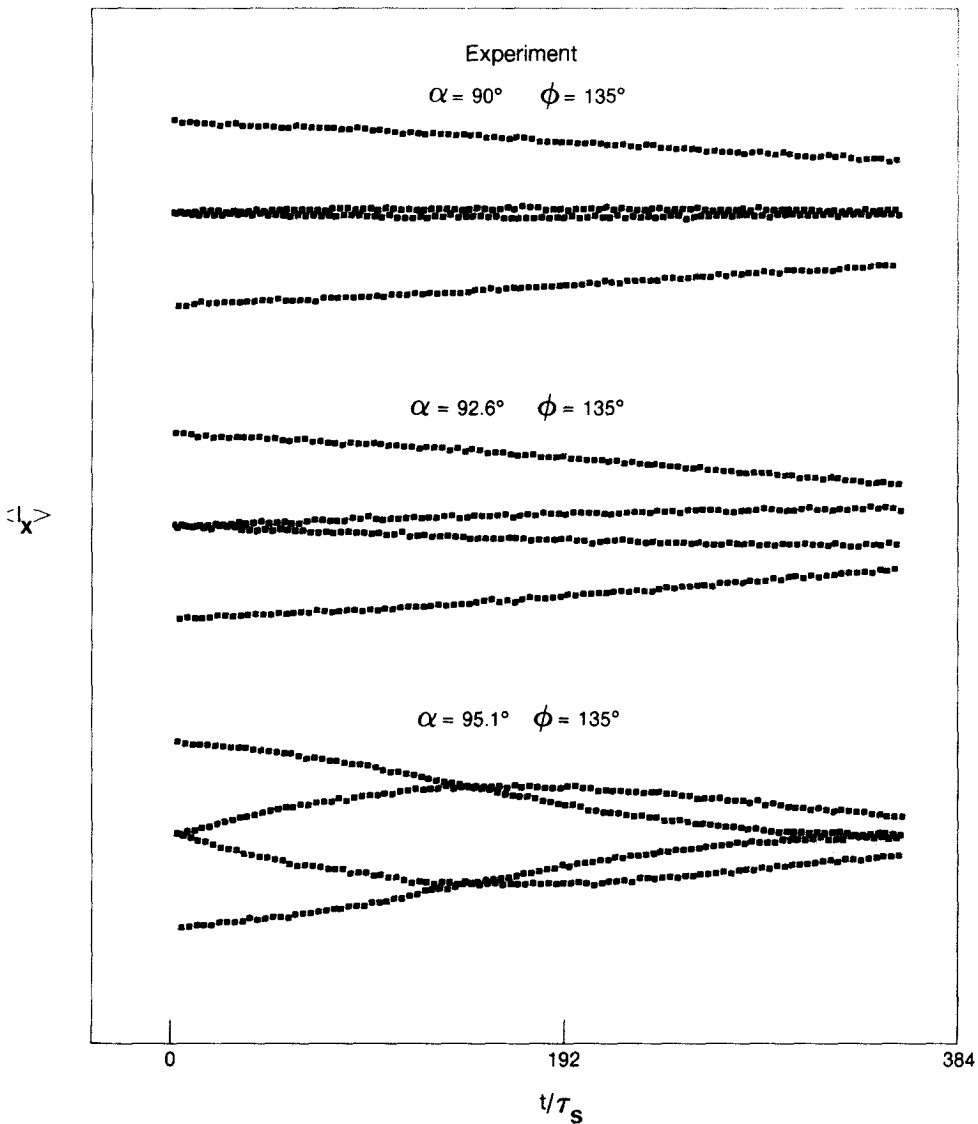


FIG. 5. Experimental results obtained with the sequence of Fig. 1a and a nominal  $135^\circ$  phase shift. The time-domain signal is quite insensitive to misadjustment of the  $90^\circ$  pulse lengths, showing excellent compensation for RF inhomogeneity.

olution and operator patience. For very small increments (large  $q$ ) the number of "lines" predicted for the time-domain signal is impractically large. In such a case one may resort to computer simulation of the multiple-pulse FID: as the figures show, once the  $\omega_1$  distribution has been determined, computer simulation of the time-domain signal yields an accurate determination of the phase shift. Direct Fourier transformation of the signal, possibly using the sequence of Fig. 1b, provides an alternative way to measure the phase. Increased compensation for RF inhomogeneity manifests

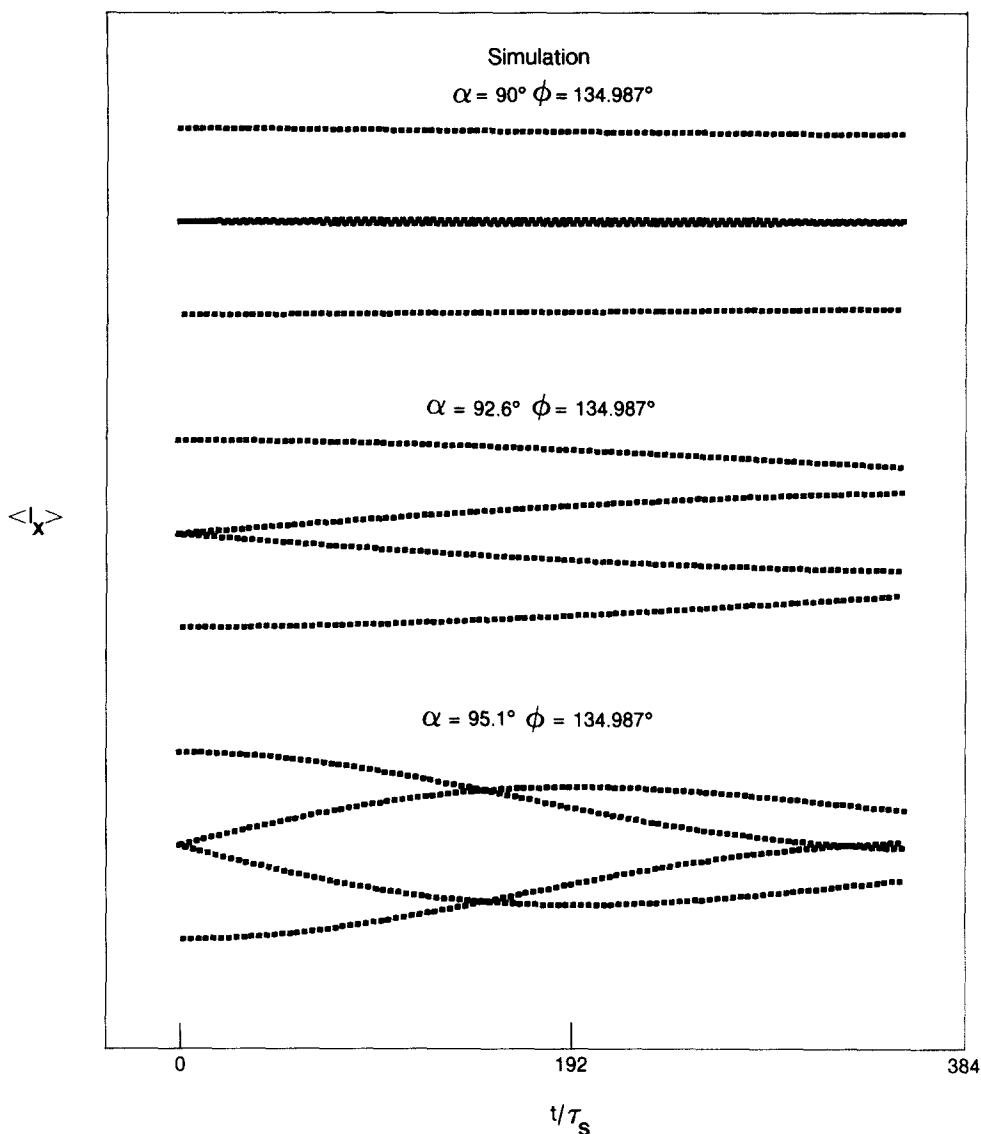


FIG. 6. Simulated multiple-pulse FIDs corresponding to the experimental data shown in Fig. 5. Best agreement is obtained for a phase setting  $\phi = 134.987^\circ$ , showing considerably less systematic error than in the case of nominal  $45^\circ$  phase shifts.

itself as a narrower resonance and hence reduced phase uncertainty, so the precision of the Fourier method should be correspondingly high.

#### CONCLUSIONS

We have shown that RF phase shifts can be very precisely measured and accurately calibrated using the nuclear spins themselves to monitor the phase of the RF field. The sequences proposed here successfully eliminate the influence of other imperfections to a large extent, so that the behavior of the spins is dominated by a nutation

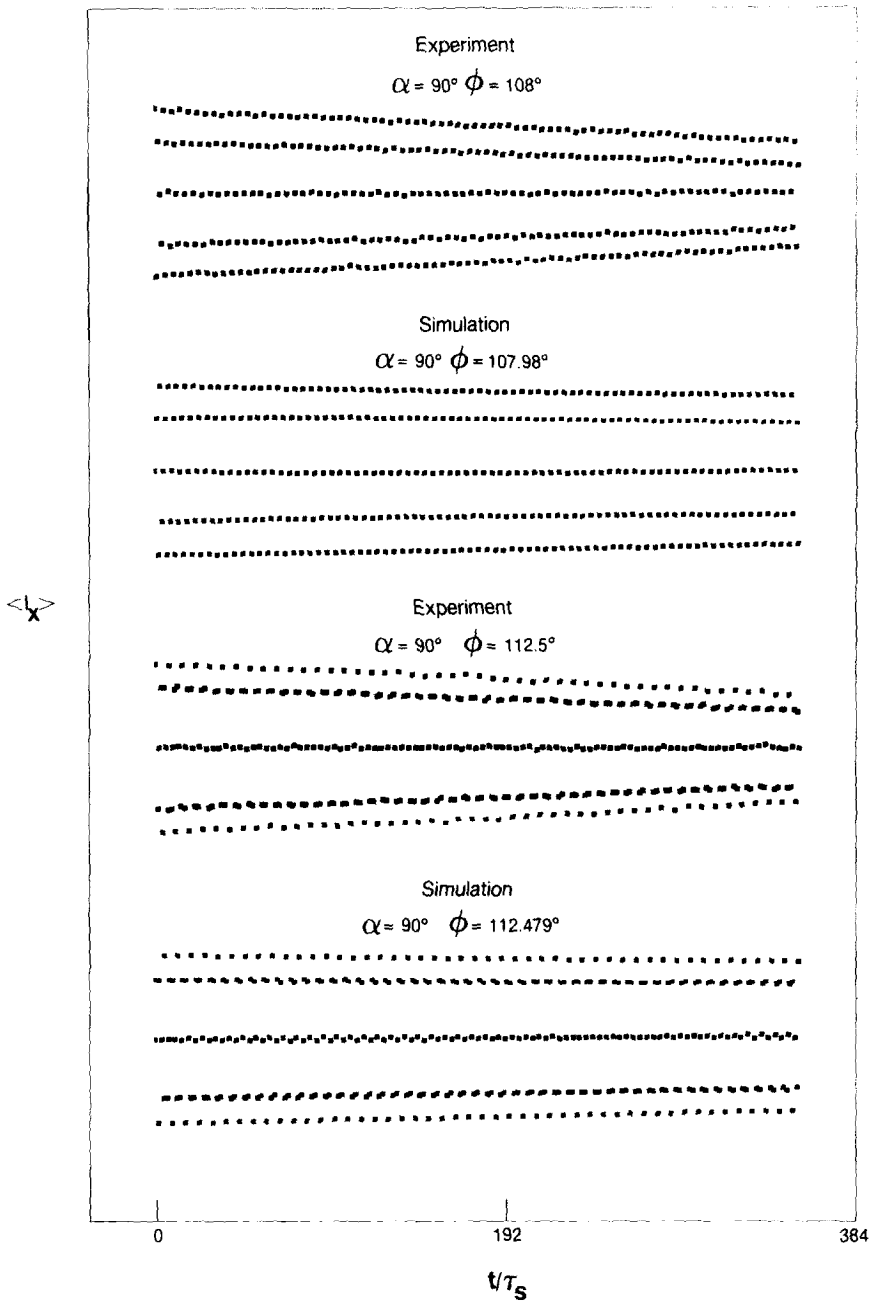


FIG. 7. Rational fractions of  $\pi$  phase shifts give rise to systematic patterns, as shown above. Both  $\phi = 108^\circ$  ( $3\pi/5$ ) and  $\phi = 112.5^\circ$  ( $5\pi/8$ ) give pleasing five-line patterns. The simulated multiple-pulse FIDs give best agreement for  $\phi = 107.98^\circ$  and  $\phi = 112.479^\circ$ , respectively, a systematic error of about  $0.02^\circ$ .

depending only on the relative phase of the RF pulses. We expect these sequences to be of practical value in aligning transmitter phases, and in devising automated algorithms for phase alignment under computer control.

## ACKNOWLEDGMENTS

This work has been supported by the Director, Office of Energy Research, Material Science Division of the U.S. Department of Energy, under Contract DE-AC03-76SF00098. A.J.S. acknowledges the support of the Miller Foundation, and stimulating discussions with Dr. Alec Norton.

## REFERENCES

1. A. BAX, "Two-Dimensional NMR in Liquids," Delft Univ. Press, Reidel, Dordrecht/Boston/London, 1982.
2. A. WOKAUN, G. BODENHAUSEN, AND R. R. ERNST, "Principles of NMR in One and Two Dimensions," Oxford Univ. Press, Oxford, 1987.
3. M. H. LEVITT AND R. FREEMAN, *J. Magn. Reson.* **33**, 473 (1979).
4. R. FREEMAN, S. P. KEMPEL, AND M. H. LEVITT, *J. Magn. Reson.* **38**, 453 (1980).
5. M. H. LEVITT, *J. Magn. Reson.* **48**, 234 (1982).
6. M. H. LEVITT, *J. Magn. Reson.* **50**, 95 (1982).
7. A. J. SHAKA AND R. FREEMAN, *J. Magn. Reson.* **55**, 487 (1983).
8. A. J. SHAKA AND R. FREEMAN, *J. Magn. Reson.* **59**, 169 (1984).
9. R. TYCKO, *Phys. Rev. Lett.* **51**, 775 (1983).
10. R. TYCKO, E. SCHNEIDER, AND A. PINES, *J. Chem. Phys.* **81**, 680 (1984).
11. R. TYCKO, H. M. CHO, E. SCHNEIDER, AND A. PINES, *J. Magn. Reson.* **61**, 90 (1985).
12. M. H. LEVITT, *Prog. NMR Spectrosc.* **18**, 61 (1986).
13. U. HAEBERLEN, "High Resolution NMR in Solids, Selective Averaging," Academic Press, New York, 1976.
14. U. HAEBERLEN AND J. S. WAUGH, *Phys. Rev.* **175**, 453 (1968).
15. J. S. WAUGH, L. HUBER, AND U. HAEBERLEN, *Phys. Rev. Lett.* **20**, 180 (1968).
16. P. MANSFIELD, *J. Phys. C* **4**, 1444 (1971).
17. W.-K. RHIM, D. D. ELLEMAN, AND R. W. VAUGHAN, *J. Chem. Phys.* **59**, 3740 (1973).
18. W.-K. RHIM, D. D. ELLEMAN, L. B. SCHREIBER, AND R. W. VAUGHAN, *J. Chem. Phys.* **60**, 4595 (1974).
19. D. P. BURUM AND W.-K. RHIM, *J. Chem. Phys.* **71**, 944 (1979).
20. D. P. BURUM, M. LINDER, AND R. R. ERNST, *J. Magn. Reson.* **44**, 173 (1981).
21. Y. S. YEN AND A. PINES, *J. Chem. Phys.* **78**, 3579 (1983).
22. (a) J. BAUM, M. MUNOWITZ, A. N. GARROWAY, AND A. PINES, *J. Chem. Phys.* **83**, 2015 (1985).
22. (b) A. N. GARROWAY, *J. Magn. Reson.* **63**, 504 (1985).
23. J. BAUM AND A. PINES, *J. Am. Chem. Soc.* **108**, 7447 (1986).
24. J. BAUM, K. K. GLEASON, A. PINES, A. N. GARROWAY, AND J. REIMER, *Phys. Rev. Lett.* **56**, 1377 (1986).
25. M. MUNOWITZ AND A. PINES, *Adv. Chem. Phys.* **66**, 1 (1987).
26. U. HAUBENREISSER AND B. SCHNABEL, *J. Magn. Reson.* **35**, 175 (1979).
27. S. IDZIAK AND U. HAEBERLEN, *J. Magn. Reson.* **50**, 281 (1982).
28. D. P. BURUM, M. LINDER, AND R. R. ERNST, *J. Magn. Reson.* **43**, 463 (1981).
29. M. MEHRING, "High Resolution NMR Spectroscopy in Solids," Springer-Verlag, Berlin/Heidelberg/New York, 1976.
30. M. MEHRING AND J. S. WAUGH, *Rev. Sci. Instrum.* **43**, 649 (1972).
31. J. D. ELLETT, M. G. GIBBY, U. HAEBERLEN, L. M. HUBER, M. MEHRING, A. PINES, AND J. S. WAUGH, in "Advances in Magnetic Resonance" (J. S. Waugh, Ed.), Vol. 5, p. 117, Academic Press, New York, 1971.
32. R. W. VAUGHAN, D. D. ELLEMAN, L. M. STACEY, W.-K. RHIM, AND J. W. LEE, *Rev. Sci. Instrum.* **43**, 1356 (1972).